Phase Noise Measurements of AlN Contour-Mode Resonators

Etienne Vaillant, Fabrice Sthal, Joël Imbaud,
Valérie Petrini, Philippe Abbe, Lilia Arapan,
F. X. Esnault[*], G. Cibiel[*]
FEMTO-ST Institute
UFC, CNRS, ENSMM, UTBM, UBFC
Besançon, France
[*]CNES, Toulouse, France
fsthal@ens2m.fr

Gianluca Piazza, Jeronimo Segovia-Fernandez
Department of Electrical and Computer Engineering
Carnegie Mellon University
Pittsburgh, Pennsylvania, USA, 15213
Email: piazza@ece.cmu.edu

Abstract—**In this paper, passive measurement system is used to explore the phase noise of aluminum nitride contour mode resonators. Their resonant frequencies are around 220 MHz. The carrier suppression technique is used. The noise floor of the measurement system is around -135 dBc/Hz @ 1 Hz offset from the carrier. Then, measurements of several resonators are presented and discussed.**

Keywords—1/f noise; resonator; AlN; contour-mode resonators; microelectromechanical systems (MEMS) resonators; phase noise; carrier suppression technique.

I. INTRODUCTION

Many laboratories develop currently resonators dedicated to time bases by means of collective process and using microtechnologies [1-6]. Some of the oscillators produced by these MEMS technologies could be perturbed by the inherent noise of the resonator which limits performances. The Carnegie Mellon University in Pittsburgh made the choice of technologies in AlN piezoelectric thin film using contour vibrating modes that are compatible with CMOS integration technologies [7]. In this paper, we propose to measure the inherent noise of these acoustic resonators without the associated oscillator. The main principle of these set-ups is the carrier suppression method. The resonant frequency of this type of resonator is set by the width of the finger and the acoustic velocity of the resonator stack. Characterization of 220 MHz aluminum nitride contour-mode resonators (CMR) is given and discussed (Fig. 1).
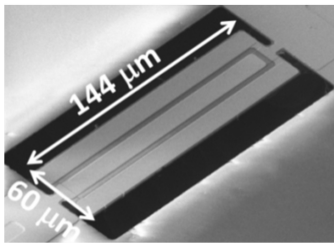

Fig. 1. Scanning electron micrograph of typical 220 MHz AlN contour-mode resonator fabricated at CMU and characterized in this study.

A set of four AlN CMRs have been tested and measured. First, the intrinsic parameters of these resonators are presented.

Then the transfer function of the packaged devices is shown in order to evaluate their loaded quality factor. Finally, results of phase noise measurement are summarized.

II. RESONATORS CHARACTERISTICS

The electrical model to describe the resonance response of AlN CMRs is given in Fig. 2. It is the usual model of a quartz crystal resonator.
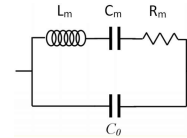

Fig. 2. Electrical model of an AlN CMR resonator whose motional parameters are L_m, R_m, C_m and C_0.

Impedance response has been measured for a set of four resonators in order to evaluate their intrinsic quality factors. Impedance plots are shown in Fig. 3. Each letter G, I, L and N corresponds to a different resonator.
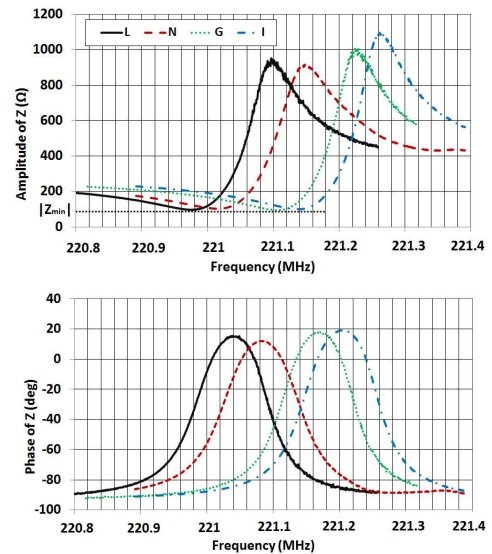

Fig. 3. Tested impedance response Z (amplitude (top) and phase) of four AlN CMR resonators.

Motional parameters of these resonators are given in Table I.

TABLE I.   MOTIONAL PARAMETERS OF THE ALN CONTOUR-MODE RESONATORS

Res.	R_m (Ω)	L_m (mH)	C_m (fF)	C_0 (pF)	Q	$f_{res.(|Zmin|)}$ (MHz)
I	110	0.269	1.93	2.14	3 398	221.140
L	109	0.258	2.01	2.37	3 286	220.980
G	106	0.264	1.96	2.30	3 473	221.100
N	116	0.257	2.02	2.26	3 077	221.020

The motional parameters are computed by the impedance analyzer (4395A) according the equivalent circuit (Fig. 2). The motional resistance is about 100 Ω. The Q factors have been calculated using the equation (1) and are around 3 000 which fits with previous publication [7].

$$Q = \frac{2\pi \cdot f_{res.} \cdot L_m}{R_m} \qquad (1)$$

III.   CONDITIONING OF RESONATORS

To reduce the impact of thermal fluctuations, the chip containing the four resonators was glued into a TO8 package. The four resonators have been bonded in separate pins. The TO8 package is then inserted into an oven. The temperature was fixed around 55°C. The purpose of this setup was not to get the turnover point, but to avoid environmental temperature fluctuations. A picture of the oven is shown in Fig. 4.

Fig. 4.   Oven used to stabilize the external temperature around 55°C.

The motional resistor of all the tested AlN CMRs is around 100 Ω. As the oven's impedance is adapted upstream and downstream, it is important to adjust this adaptation at the input of the Device Under Test (DUT) inside the oven, as shown in Fig. 5.
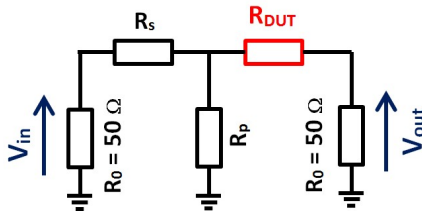

Fig. 5.   Impedance matching for resonators.

R_s and R_p are around 30 Ω and 20 Ω respectively. The loaded quality factor has been calculated from the transfer function obtained with the Network Analyzer. This measurement has been done between the input and output of the oven. Consequently every component and cable inside the oven took part in the measurement. At the resonant frequency the loss induced by the resonators is around 15 dB and the loaded quality factor has been estimated around 1 200 for the four tested resonators (details in Table II). This resonator set-up is used for the noise measurement and the loaded Q values are used to estimate the flicker floor in term of Allan standard deviation [8].

The Leeson frequency F_L can be defined according to (2):

$$F_L = \frac{1}{\frac{\Delta\emptyset}{\Delta f}_{\pm 1°}} \qquad (2)$$

where $\frac{\Delta\emptyset}{\Delta f}$ is the slope of the phase at the resonant frequency of the resonator, converted in rad/Hz. The Q factor is then calculated using the following expression:

$$Q_L = \frac{f_{res}}{2 \cdot F_L} \qquad (3)$$

TABLE II.   LOADED Q FACTOR AND LOSS AT RESONANCE OF THE RESONATORS

Res.	I	L	G	N
Loss (dB)	15.4	15.2	15	15.5
Phase slope (10^{-6} rad/Hz)	9.68	10.3	11.4	10.6
F_L (Hz)	103 200	97 087	87 719	94 340
Q_L	1 071	1 138	1 260	1 171

IV.   MEASUREMENT SYSTEM

The passive technique using carrier suppression is used to characterize the inherent phase stability of the resonators [8]. The principle of the carrier suppression bench is shown in Fig. 6. The general idea of this passive method consists in reducing the noise of the source as much as possible. This suppression is obtained by a first stage where signals of both ways are subtracted and then the resulting signal is amplified. More precisely a part of the source signal is separated in two equal parts in order to drive the DUT. The DUT can be either a resistor allowing the calibration of the system so as to establish its resolution, or a resonator whose phase noise is sought. The attenuation of the DUT is compensated by an attenuator in the second arm. After that the two signals are vectorially added with a 180° phase shift. The carrier suppression is done with a power splitter (0° to 180°) before the classical phase detection. Obtaining high carrier suppression requires a fine adjustment of both amplitude and phase of the two signals.

The resulting signal is highly amplified without saturation of the amplifier (of gain β). This signal is then subjected to the phase detection mixing with the input signal in phase quadrature and then amplified (gain β') to be higher than the noise floor of the Fast Fourier (FFT) spectrum analyzer.
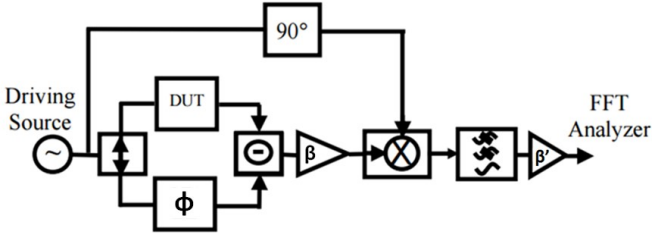
Fig. 6. Principle of the carrier suppression technique.

A picture of our implementation is shown in Fig. 7. Calibration of the measurement system is obtained by injecting a known sideband on one of the arms of the bridge. This sideband simulates an equivalent phase noise. The result of the measurement is corrected using the calibration factor determined from this sideband.
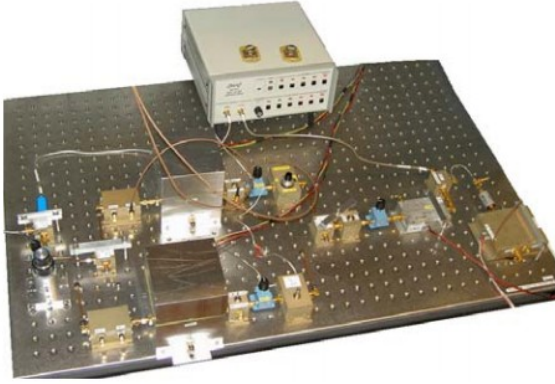

Fig. 7. Carrier Suppression technique setup.

The noise floor of the system is presented at 221 MHz in Fig. 8. The system exhibits a $\mathcal{L}(1Hz)$ around -136 dBc/Hz, $\mathcal{L}(10Hz)$ = -148 dBc/Hz and then a thermal floor near -154 dBc/Hz. For this noise floor measurement a resistor has been used instead of a resonator. The dissipated power by the resistor is about 140 µW.
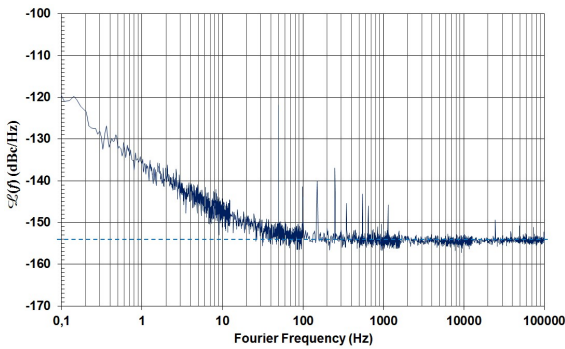

Fig. 8. Noise floor of the measuremnt system at 221 MHz.

The driving source was coming from a 1 GHz Cryogenic Sapphire Oscillator (CSO) signal divided by a Direct Digital Synthesizer (DDS, AD9912). The advantage of a DDS is the possibility to adjust the frequency with a very high resolution in order to get the resonant frequencies of the resonators.

V. PRELIMINARY RESULTS

A measured example of the single sideband Power Spectral Density (PSD) of phase fluctuation, $\mathcal{L}(f)$, is presented in Fig. 9. The drive level power dissipated by the resonator is about 140 µW. The noise of the resonator is at least 10 dB above the noise floor of the system, as measured by using a resistor instead of the resonator. We can observe the $1/f$ noise of the resonator. In this case, the loaded Q is about 1200, then, the cut-off frequency F_L is close to 90 kHz. Thus the filter part in $1/f^3$ slope is not visible and it is hidden by the noise floor of the measurement system.

The best resonator shows a phase noise of -125 dBc/Hz at 1 Hz offset from the carrier. A summary of the phase noise measurement results for the four AlN devices is given in Table III. The resonators have been measured with different driving powers: 35, 70 and 140 µW. In this kind of measurement the error in the determination of $\mathcal{L}(f)$ is usually ±2 dB because of the FFT analyzer precision. The measured noise given by the passive measurement can be transformed into equivalent oscillator noise (b'_{-3} (dBrad²/Hz)) and into Allan standard deviation (σ_{y_floor} (10^{-9})) [9].

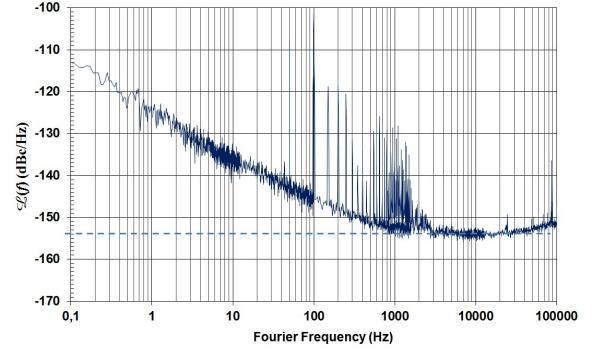Fig. 9. Power spectral density of the phase fluctuations of a AlN contour mode resontaor, dissipated power is around 140 µW.

TABLE III. NOISE RESULTS OF SEVERAL AlN CMRs FOR THREE DIFFERENT DISSIPATED POWERS

Power	35 µW			
Res.	I	L	G	N
Q_L	1071	1138	1260	1171
$\mathcal{L}(1\,Hz)$ dBc/Hz	-125	-115	-118	-117
$S_\phi(1Hz)$ (dBrad²/Hz)	-122	-112	-115	-114
b'_{-3} (dBrad²/Hz)	-21.7	-12.3	-16.2	-14.6
$\sigma_{y\,floor}$ (10^{-9})	0.44	1.30	0.83	0.99

Power	70 µW			
Res.	I	L	G	N
Q_L	1071	1138	1260	1171
$\mathcal{L}(1\,Hz)$ dBc/Hz	-120	-117	-115	-113
$S_\phi(1Hz)$ (dBrad²/Hz)	-117	-114	-112	-110
b'_{-3} (dBrad²/Hz)	-16.7	-14.3	-13.2	-9.6
$\sigma_{y\,floor}$ (10^{-9})	0.77	1.03	1.17	1.76

Power	140 µW			
Res.	I	L	G	N
Q_L	1071	1138	1260	1171
$\mathcal{L}(1\,Hz)$ dBc/Hz	-125	-113	-112	-113
$S_\phi(1Hz)$ (dBrad²/Hz)	-122	-110	-109	-110
b'_{-3} (dBrad²/Hz)	-21.7	-13.3	-10.2	-9.6
$\sigma_{y\,floor}$ (10^{-9})	0.44	1.15	1.65	1.76

One of the tested resonators exhibits a flicker floor of about 10^{-10}. The others are more close to 10^{-9}. In this set of experiment the driving power dependence of the resonator noise is not clearly shown. Further investigation will be necessary to conclude about this last point. Another perspective of this work is to measure several other AlN resonators and to use them in an oscillator circuit.

VI. CONCLUSION

Phase noise of Aluminum Nitride Contour Mode Resonators has been explored using a passive measurement system with carrier suppression. The $1/f$ noise of acoustic resonators is clearly shown. These resonators present a good short-term stability around few 10^{-9} - 10^{-10} which is in the same order of magnitude than usual TCXO.

ACKNOWLEDGMENT

REFERENCES

[1] T. L. Naing, T. O. Rocheleau, E. Alon, C. Nguyen, A "78-μW GSM Phase Noise-Compliant Pierce Oscillator Referenced to a 61-MHz Wine-Glass Disk Resonator", in Proc. IEEE Int. Freq. Contr. Symp., pp. 562-565, 2013.

[2] G. Piazza, A. Tazzoli, N. Miller, J. Segovia, C. Cassella, J. Koo, B. Otis, K. McNaul, B. Gibson, K. Turner, T. Palmer, "Dynamics of Microscale Thin Film AlN Piezoelectric Resonators Enables Low Phase Noise UHF Frequency Sources", in Proc. IEEE Int. Freq. Contr. Symp., pp. 555-558, 2013

[3] R.G. Nagele, H.P. Moyer, D. J. Kirby, Y. Yoon, R. L. Kubena, R. J. Joyce, P. D. Brewer, D. T. Chang, "A 995 MHz Fundamental Nonlinear Quartz MEMS Oscillator", in Proc. IEEE Int. Freq. Contr. Symp., pp. 566-570, 2013.

[4] M.E. Ivan, B. Dulmet, G. Martin, P. Abbe, L. Robert, S. Ballandras, "New electrostatically-excited single crystal silicon resonator vibrating in a Thickness-Extensional mode", in Proc. IEEE Int. Freq. Contr. Symp., pp. 743-748, 2012.

[5] T. Barron, D. Gachon, G. Martin, S. Alzuaga, D. Hermelin, J.P. Romand, S. Ballandras, "Temperature Compensated Radio-Frequency Harmonic Bulk Acoustic Resonators", in Proc. IEEE Int. Freq. Contr. Symp., pp. 652-655, 2012.

[6] P. Varshney, B. S. Panwar, P. Rathore, S. Balandras, B. François, G. Martin, J. M. Friedt, T. Retornaz, "Theoretical and experimental analysis of high Q SAW resonator transient response in a wireless sensor interrogation application", in Proc. IEEE Int. Freq. Contr. Symp., pp. 451-456, 2012.

[7] N. Miller, G. Piazza, "Measurements of Frequency Fluctuations in Aluminum Nitride Contour-Mode Resonators", IEEE Transactions on Ultrasonics, Ferroelectrics and Frequency Control, vol. 61, no. 6, June, pp. 913-919, 2014.

[8] F. Sthal J. Imbaud, X. Vacheret, P. Salzenstein, G. Cibiel, S. Galliou, "Computation Method for the Short-Term Stability of Quartz Crystal Resonators Obtained From Passive Phase Noise Measures", IEEE Transactions on Ultrasonics, Ferroelectrics and Frequency Control, vol. 60, no. 7, July, pp. 1530-1532, 2013.

[9] E. Rubiola, "Phase noise and frequency stability in oscillators", Cambridge University Press, 2009.